

Original Research

Multi-Omics Characteristics of Ferroptosis Associated with Colon Adenocarcinoma Typing and Survival

Xiao-Qiong Chen^{1,*}, Ke Lian^{1,†}, Zi-Wei Chen^{1,†}, Xuan Zhang¹, Ting Li¹, Tao Wu¹,
Tao Shen¹, Xin-Yi Cai¹, Xian-Shuo Cheng¹, Fu-Hui Xiao², Yun-Feng Li^{1,*}¹Colorectal Surgery, Third Affiliated Hospital of Kunming Medical University, Yunnan Cancer Hospital, 650000 Kunming, Yunnan, China²State Key Laboratory of Genetic Resources and Evolution, Kunming Institute of Zoology, Chinese Academy of Sciences, 650000 Kunming, Yunnan, China*Correspondence: chenxiaoduoycc@126.com (Xiao-Qiong Chen); liyunfeng001@foxmail.com; liyunfeng@medmail.com.cn (Yun-Feng Li)

†These authors contributed equally.

Academic Editor: Ricardo Jorge Pinto Araujo

Submitted: 28 June 2023 Revised: 26 November 2023 Accepted: 21 December 2023 Published: 17 January 2024

Abstract

Background: Ferroptosis, an iron-dependent form of cell death, plays a crucial role in the progression of various cancers, including colon adenocarcinoma (COAD). However, the multi-omics signatures relevant to ferroptosis regulation in COAD diagnosis remain to be elucidated. **Methods:** The transcriptomic, miRNAomic, and methylomic profiles of COAD patients were acquired from the Cancer Genome Atlas (TCGA). Ferroptosis activity in these patients was determined, represented by a ferroptosis score (FS), using single-sample gene set enrichment analysis (ssGSEA) based on the expression of ferroptosis-related genes. **Results:** Results showed that the COAD patients with high-FS displayed favorable survival outcomes and heightened drug sensitivity. They also exhibited an up-regulation of genes involved in immune-related pathways (e.g., tumor necrosis factor signaling pathway), suggesting a correlation between immunity and ferroptosis in COAD progression. Furthermore, three survival prediction models were established based on 10 CpGs, 12 long non-coding RNAs (lncRNAs), and 14 microRNAs (miRNAs), respectively. These models demonstrated high accuracy in predicting COAD survival, achieving areas under the curve (AUC) >0.7. The variables used in the three models also showed strong correlations at different omics levels and were effective at discriminating between high-FS and low-FS COAD patients (AUC >0.7). **Conclusions:** This study identified different DNA methylation (DNAm), lncRNA, and miRNA characteristics between COAD patients with high and low ferroptosis activity. Furthermore, ferroptosis-related multi-omics signatures were established for COAD prognosis and classification. These insights present new opportunities for improving the efficacy of COAD therapy.

Keywords: colon adenocarcinoma; ferroptosis; multi-omics; oncology; diagnostic signature

1. Introduction

Colon adenocarcinoma (COAD), a prevalent malignant cancer globally [1,2], continues to exhibit an upward trend in both incidence and mortality rates [3,4]. A major obstacle in COAD diagnosis and therapy is its pronounced heterogeneity at different molecular levels [5,6]. Early detection and intervention are crucial, as they substantially enhance patient survival prospects [1,7]. Consequently, the need for research focused on the identification of diagnostic and classification biomarkers for COAD remains critical.

Ferroptosis, characterized as an oxidative and iron-dependent form of regulated cell death, plays a significant role in the development of various cancers, such as breast cancer, hepatocellular carcinoma, and COAD [8–12]. Emerging evidence suggests a strong association between ferroptosis and various molecular factors, including messenger RNA (mRNA), long non-coding RNA (lncRNA), microRNA (miRNA), along with epigenetic modifications like DNA methylation (DNAm), in tumor progression [13–15]. Alterations in the expression of ferroptosis-related mRNA genes have been instrumental

in cancer prognosis prediction, including COAD [9,12,16]. However, a comprehensive exploration of ferroptosis-associated signatures, particularly in relation to COAD classification and diagnosis, at other molecular levels has not yet been fully explored.

In this study, transcriptomic, miRNomic, methylomic, and clinical data of COAD patients were obtained from the Cancer Genome Atlas (TCGA). The ferroptosis score (FS) of each COAD patient was calculated based on the expression of 20 ferroptosis-associated genes using single-sample gene set enrichment analysis (ssGSEA). The COAD patients were then classified into either high-FS or low-FS subtypes, with the high-FS group demonstrating better survival probability and heightened sensitivity to multiple anti-cancer drugs. Additionally, 1065 differentially expressed mRNAs (DE-mRNAs), 324 differentially expressed lncRNAs (DE-lncRNAs), 91 differentially methylated CpG sites (DMCs), and 39 differentially expressed miRNAs (DE-miRNAs) were identified between the high-FS and low-FS COAD groups. Notably, the up-regulated protein-coding mRNAs in the high-FS COAD patients were enriched in



immune-related pathways. Three ferroptosis-related signatures comprising 10 DMCs, 12 DE-lncRNAs, and 14 DE-miRNAs were constructed using the least absolute shrinkage and selection operator (LASSO) Cox regression model, yielding a high degree of accuracy in the prediction of COAD prognostic outcomes. Further mixOmics analysis revealed that the ferroptosis-related multi-omics features displayed excellent performance in COAD classification.

2. Methods

2.1 Data Collection and Preprocessing

RNA-seq (HTSeq-Counts/log₂(FPKM+1)), Illumina Human Methylation 450K BeadChip (HM450, β -value), miRNA-seq (log₂(TPM)), and clinical data of COAD and normal samples were downloaded from the TCGA database using the UCSC Xena platform (<https://xena.ucsc.edu/>). The transcriptome dataset included 446 COAD samples and 39 normal samples, the methylome dataset included 297 COAD samples and 18 normal samples, and the miRNAome dataset included 425 COAD samples and seven normal samples. The expression levels of mRNAs, lncRNAs, and miRNAs were transformed into FPKM and TPM values. Gene expression microarray data for COAD were downloaded from the Gene Expression Omnibus (GEO) database (GSE39582) [17]. The matrix of each dataset was normalized using the ‘normalize.quantiles’ function in the R “preprocessCore” (v1.64.0) package (<https://bioconductor.org/>).

2.2 Inferred FS

In total, 288 ferroptosis-related genes, including drivers, suppressors, and markers were obtained from the FerrDb database [18]. Among them, genes with relationships between expression and COAD survival were identified using univariate Cox survival analysis. The ssGSEA function in the R package “GSVA” (v1.50.0) (<https://bioconductor.org/>) was used to calculate the enrichment scores of gene sets positively or negatively associated with COAD survival [19]. The FS, representing the ferroptosis level in each COAD sample, was defined as the difference in enrichment scores between positive and negative components.

2.3 Sensitivity Analysis of Drug Reactions in COAD Patients

Cancer cell line drug sensitivity data (IC₅₀) were downloaded from the Genomics of Drug Sensitivity in Cancer database (GDSC, <https://www.cancerrxgene.org/>) [20,21]. The drug sensitivity score of each COAD patient was estimated using the R package “oncoPredict” (v0.2) (<https://cran.r-project.org/>) based on gene expression data [22]. Drugs with a mean predicted sensitivity value ≤ 0.5 in patients were retained. Differences in response sensitivity for each drug between the two groups were tested using Student’s *t*-test. Correlations between ferroptosis scores (FSs)

and estimated drug sensitivity scores were determined using Pearson correlation analysis. A *p*-value < 0.05 was considered statistically significant.

2.4 Survival Analysis

Survival differences between the two groups were calculated using the Kaplan-Meier method and log-rank test in the R package “survival” (v3.5-7) (<https://cran.r-project.org/>). Samples were classified into two subgroups based on the median FS or risk score values.

2.5 DE-mRNA, DE-lncRNA, DMC, and DE-miRNA Analyses

DE-mRNAs and DE-lncRNAs were identified using the R package “DESeq2” (v1.42.0) (<https://bioconductor.org/>) based on the thresholds: $|\log_2\text{Fold-change}| > 1$ and adjusted $p < 0.01$ between the tumor and normal groups and $|\log_2\text{Fold-change}| > 0.5$ and adjusted $p < 0.01$ between the high-FS and low-FS COAD subgroups. DE-miRNAs were identified using the R package “limma” (v3.58.1) (<https://bioconductor.org/>) based on the thresholds: adjusted $p < 0.01$ between the tumor and normal groups and adjusted $p < 0.01$ between the high-FS and low-FS COAD subgroups. DMCs were also identified using the R package “limma” based on the thresholds: $|\text{methylation difference}| > 0.2$ and adjusted $p < 0.01$ between the tumor and normal groups and $|\text{methylation difference}| > 0.1$ and adjusted $p < 0.01$ between the high-FS and low-FS COAD subgroups.

2.6 Biological Function Enrichment Analysis

Gene Ontology (GO) and Kyoto Encyclopedia of Genes and Genomes (KEGG) pathway enrichment analyses were performed for the DE-mRNAs using DAVID (<https://david.ncifcrf.gov/tools.jsp>) [23]. A Benjamini-Hochberg (BH)-adjusted *p*-value < 0.05 was considered statistically significant.

2.7 Construction of Multi-Omics Prognostic Signatures

LASSO Cox regression model analysis was used for variable selection with the “glmnet” R package. Multivariate analysis based on the Cox proportional hazards regression model was used to calculate the coefficients of the selected variables and construct the prognostic signatures. Receiver operating characteristic (ROC) curves and area under the ROC curves (AUC) were used to evaluate the effectiveness of the prognostic model with the “survival-ROC” R package (v1.0.3.1) (<https://cran.r-project.org/>).

2.8 Discriminant Analysis

The “mixOmics” R package was employed to select key variables within the three -omics data signatures that effectively differentiate between the high-FS and low-FS COAD subgroups according to the provided instructions (<http://mixomics.org/>) [24]. In brief, the continuous quantitative values of variables, such as the expression levels

Table 1. Clinical characteristics of COAD patients.

Characteristic	Number (%)	HR (95% CI)	<i>p</i> -value
Age		1 (1–1)	0.041
<60	125		
>60	309		
Sex		1.6 (0.95–2.5)	0.074
Female	207		
Male	239		
Stage		2.1 (1.6–2.8)	3×10^{-7}
Stage I	76		
Stage II	171		
Stage III	126		
Stage IV	62		

HR, hazard ratio; CI, confidence interval.

of lncRNAs and miRNAs and methylation levels of CpGs, within the three signatures served as input data for the “mixOmics” package (v6.26.0) (<https://bioconductor.org/>). Supervised analysis and feature selection with sparse Partial Least Square-Discriminant Analysis (sPLS-DA) were performed to identify specific variables of different molecular types critical for discriminating the high-FS and low-FS groups. All statistical analyses were performed using the R program (v4.3.1) (<https://cran.r-project.org/>).

3. Results

3.1 COAD Typing Based on Inferred Ferroptosis Activity

Table 1 displays the clinical information of the 446 COAD patients and 39 normal samples. Survival analysis showed that age and pathological stage of the COAD patients were both associated with COAD survival ($p < 0.05$). Univariate Cox regression analyses identified eight ferroptosis-related genes with a positive association and 12 with a negative association between their expression and COAD survival ($p < 0.05$). The FS index of ferroptosis activity was estimated based on the expression of the 20 ferroptosis-related genes using ssGSEA (see Materials and Methods). Results showed that the FSs ranged from -0.87 to 0.65 (**Supplementary Fig. 1**). The young group (age <60 years) had higher FSs compared to the old group (age >60 years), but no significant differences in FSs were found between the male and female samples (Fig. 1A,B). Notably, FSs were lower in patients at the late pathological stage, indicating an association between FSs and tumor progression (Fig. 1C). The COAD patients were then divided into two subgroups according to median FSs. Kaplan-Meier survival analysis indicated that the high-FS patients showed good survival ($p = 0.00011$) (Fig. 1D), as validated by multivariate Cox regression analysis after correcting for age, sex, and pathological stage (Fig. 1E).

To explore the potential association between FSs and COAD treatment precision, the drug sensitivity score of each patient was calculated using the R package “oncoPredict” based on drug sensitivity data from the GDSC

database. In total, 11 agents showed sensitivity differences between the high-FS and low-FS COAD subgroups, with high drug sensitivity in the high-FS patients (Fig. 2A). Among these drugs, several have been used in COAD therapy, such as camptothecin, vinblastine, and staurosporine [25–27]. Based on further correlation analysis, 10 of the anti-cancer drugs exhibited significant associations between sensitivity and FSs (Fig. 2B).

3.2 Identifying DE-mRNAs between High- and Low-FS COAD Subgroups

Next, changes in protein-coding mRNA expression were analyzed between the two COAD subgroups. In total, 1065 DE-mRNAs exhibited differences between the COAD patients and normal samples, as well as between the high-FS and low-FS COAD subgroups (see Materials and Methods). Functional enrichment analysis of the DE-mRNAs was conducted to explore differences in biological functions and signaling pathways between the two subgroups. Notably, GO analysis identified 376 up-regulated DE-mRNAs enriched in the inflammatory response, chemokine-mediated signaling pathway, and immune response (Fig. 3A), and 689 down-regulated DE-mRNAs enriched in the Wnt signaling pathway, lipid metabolism, and cell adhesion (Fig. 3B). Furthermore, KEGG pathway analysis revealed that the up-regulated DE-mRNAs were mainly enriched in immune-related pathways, such as the TNF signaling pathway, chemokine signaling pathway, and cytokine-cytokine receptor interaction (Fig. 3C), while down-regulated DE-mRNAs were enriched in the cell adhesion molecule, chemical carcinogenesis, and cAMP signaling pathways (Fig. 3D). Therefore, these findings highlight the close association between ferroptosis and immune processes in tumor progression.

3.3 Building Ferroptosis-Related Multi-Omics Signatures for COAD Survival Prediction

Ferroptosis-related mRNA signatures associated with COAD prognosis were determined utilizing expression data of identified DE-mRNAs from the TCGA database. LASSO Cox regression analysis was performed on the 1065 DE-mRNAs, with 12 DE-mRNAs selected to build a risk model (risk-score_(mRNA)). Subsequently, the multivariate Cox model was used to calculate the coefficients, as follows:

$$\begin{aligned} \text{Risk score (mRNA)} &= (0.5975) \times ATP6V1B1 + (-0.4779) \times FZD3 + (0.8540) \times GABRD \\ &+ (-0.2871) \times GPR15 + (0.8738) \times LRRN4 + (-0.8904) \times MS4A15 \\ &+ (-2.1418) \times NRG1 + (0.2937) \times NSMF + (0.1770) \times PCOLCE2 \\ &+ (0.2700) \times PHACTR3 + (0.5333) \times PLAC1 + (0.2952) \times RSPO4 \end{aligned}$$

The risk score for each COAD patient was then calculated, with median values used to categorize patients into high- and low-risk groups. Kaplan-Meier analysis revealed a significantly poorer prognosis in the high-risk group compared to the low-risk group (Fig. 4A). The ROC curves in-

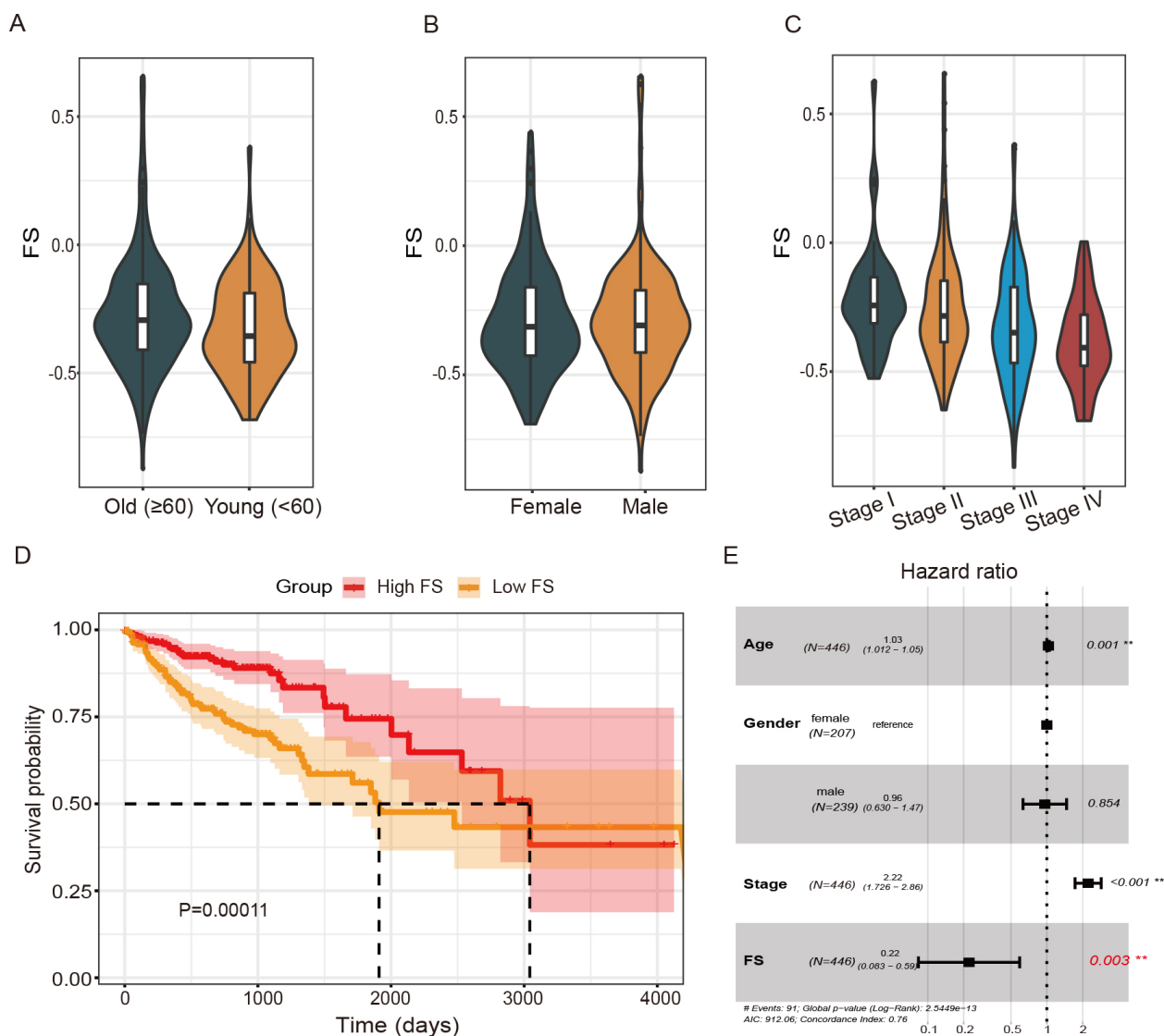


Fig. 1. Association between ferroptosis scores (FSs) and colon adenocarcinoma (COAD) overall survival. (A–C) FS differences in patients of different age, sex, and pathological stage. (D) Kaplan-Meier survival curve of high- and low-FS patients. (E) Forest plot of association between FSs and COAD survival in multivariate Cox proportional hazards model. **, $p < 0.01$, ***, $p < 0.001$.

dedicated AUC values for the risk score model at 1, 3, and 5 years of 0.833, 0.799, and 0.835, respectively (Fig. 4B). Additionally, an independent gene expression microarray dataset of COAD from the GEO database was analyzed to validate the prognostic value of the 12-DE-mRNA signature. This analysis confirmed that COAD patients with a low risk score demonstrated better survival, with AUCs of 0.582 at 3 years and 0.592 at 4 years (Fig. 4C,D). In addition, we also observed that the patients with high FS presented good survival in this independent COAD cohort (Supplementary Fig. 2).

To further explore the ferroptosis-related regulatory features associated with COAD prognostic outcomes, 91 DMCs, 324 DE-lncRNAs, and 39 DE-miRNAs were identified displaying differences between COAD patients and normal samples, as well as between the high-FS and low-

FS COAD subgroups (see Methods). A subset of 132 high-FS and 160 low-FS COAD patients with transcriptomic, miRNAomic, and methylomic data were selected for subsequent analyses. LASSO Cox regression analysis was then performed on the 91 DMCs, 324 DE-lncRNAs, and 39 DE-miRNAs to identify the most predictive features for COAD prognosis. In total, 10 DMCs, 12 DE-lncRNAs, and 14 DE-miRNAs were selected as variables for the risk score models at different molecular levels (i.e., $\text{risk-score}_{(\text{DNAm})}$, $\text{risk-score}_{(\text{lncRNA})}$, and $\text{risk-score}_{(\text{miRNA})}$). The coefficients of the selected DMCs, DE-lncRNAs, and DE-miRNAs were recalculated in each multivariate Cox model, leading to the construction of three risk prediction models (Supplementary Fig. 3), detailed as follows:

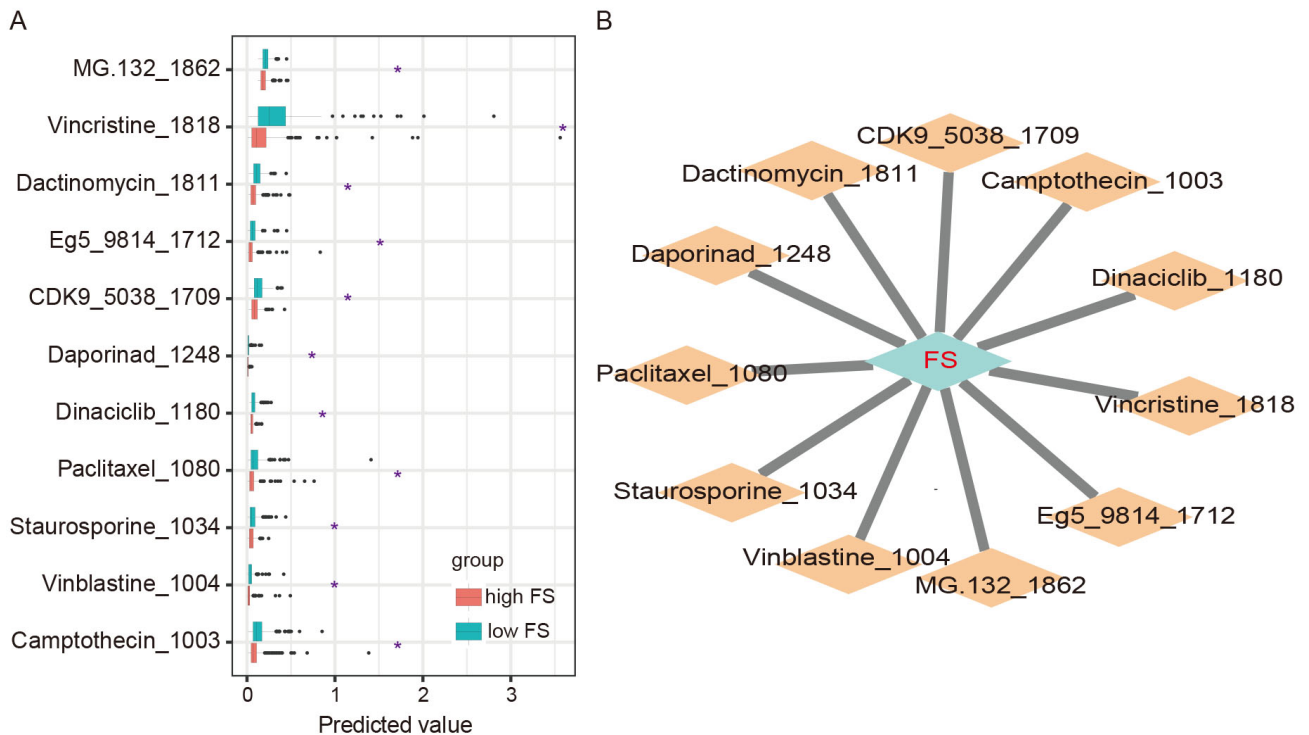


Fig. 2. Drug sensitivity between high- and low-FS COAD subgroups. (A) Differences in predicted drug sensitivity between high- and low-FS subgroups (*, $p < 0.05$). (B) Correlations between FSs and predicted sensitivity values of anti-cancer drugs in COAD patients.

$$\begin{aligned}
 \text{Risk - score (DNAm)} &= (-1.6307 \times \text{cg 00987461}) + (0.995 \times \text{cg 02415779}) \\
 &+ (-1.3444 \times \text{cg 03616722}) + (1.1853 \times \text{cg 06120945}) \\
 &+ (1.4154 \times \text{cg 14192291}) + (0.8314 \times \text{cg 15507690}) \\
 &+ (-0.8891 \times \text{cg 18693345}) + (1.1020 \times \text{cg 21308365}) \\
 &+ (-1.5025 \times \text{cg 21494776}) + (0.5229 \times \text{cg 25588389})
 \end{aligned}$$

$$\begin{aligned}
 \text{Risk - score (lncRNA)} &= (-0.46348 \times \text{AC016831.7}) + (0.51557 \times \text{ATP2A1_AS1}) \\
 &+ (1.26266 \times \text{CCDC144NL_AS1}) + (-1.69841 \times \text{RP11_109J4.1}) \\
 &+ (0.33265 \times \text{RP11_1143G9.5}) + (0.35439 \times \text{RP11_353N14.2}) \\
 &+ (-0.36330 \times \text{RP11_386I14.4}) + (0.41455 \times \text{RP11_60A8.1}) \\
 &+ (0.08611 \times \text{RP11_638I8.1}) + (0.69306 \times \text{RRP4_673M15.1}) \\
 &+ (0.14529 \times \text{RP5_1059L7.1}) + (0.55365 \times \text{RP5_884M6.1})
 \end{aligned}$$

$$\begin{aligned}
 \text{Risk - score (miRNA)} &= (0.49643 \times \text{hsa_let_7c}) + (-0.24373 \times \text{hsa_mir_144}) \\
 &+ (0.24081 \times \text{hsa_mir_146a}) + (0.20736 \times \text{hsa_mir_147b}) \\
 &+ (0.37224 \times \text{hsa_mir_16_1}) + (0.26853 \times \text{hsa_mir_217}) \\
 &+ (-0.07030 \times \text{hsa_mir_223}) + (0.13606 \times \text{hsa_mir_3074}) \\
 &+ (0.14476 \times \text{hsa_mir_33b}) + (-0.37786 \times \text{hsa_mir_3615}) \\
 &+ (-0.31860 \times \text{hsa_mir_3677}) + (-0.18818 \times \text{hsa_mir_375}) \\
 &+ (0.05530 \times \text{hsa_mir_577}) + (0.20584 \times \text{hsa_mir_625})
 \end{aligned}$$

The risk score of each COAD patient was then calculated at three molecular levels using the three different datasets. According to the median values of the risk scores inferred by each molecular signature (i.e., DNAm, lncRNA, and miRNA), the COAD patients were categorized into high- and low-risk groups (Fig. 5A,E,I). Kaplan-Meier analyses revealed significantly poorer prognosis for

patients in the high-risk group than those in the low-risk group for each -omics data type (Fig. 5B,F,J). **Supplementary Fig. 4** presents the vital statuses of COAD patients classified into the high- and low-risk groups, as determined by the signatures from the three -omics-level datasets. The risk score models from the three datasets were then used to predict patient survival status at 1, 3, and 5 years. ROC curve analysis showed that the AUC values for the DNAm risk score model were 0.725, 0.718, and 0.774 at 1, 3, and 5 years, respectively (Fig. 5C); the AUC values for the lncRNA risk score model were 0.797, 0.739, and 0.773 at 1, 3, and 5 years, respectively (Fig. 5G); and the AUC values for the miRNA risk score model were 0.717, 0.721, and 0.707 at 1, 3, and 5 years, respectively (Fig. 5K). In addition, heatmaps presented the methylation and expression level changes of the 10 DMCs, 12 lncRNAs, and 14 miRNAs within corresponding prediction models alongside their respective risk scores (Fig. 5D,H,L). Notably, a significant proportion of molecular features, including 8 DMCs, 11 lncRNAs and 8 miRNAs, demonstrated statistically significant correlations between their methylation and expression levels and the associated risk cores ($p < 0.05$; **Supplementary Table 1**). These findings suggest that ferroptosis-related multi-omics features are effective in predicting COAD prognostic outcomes.

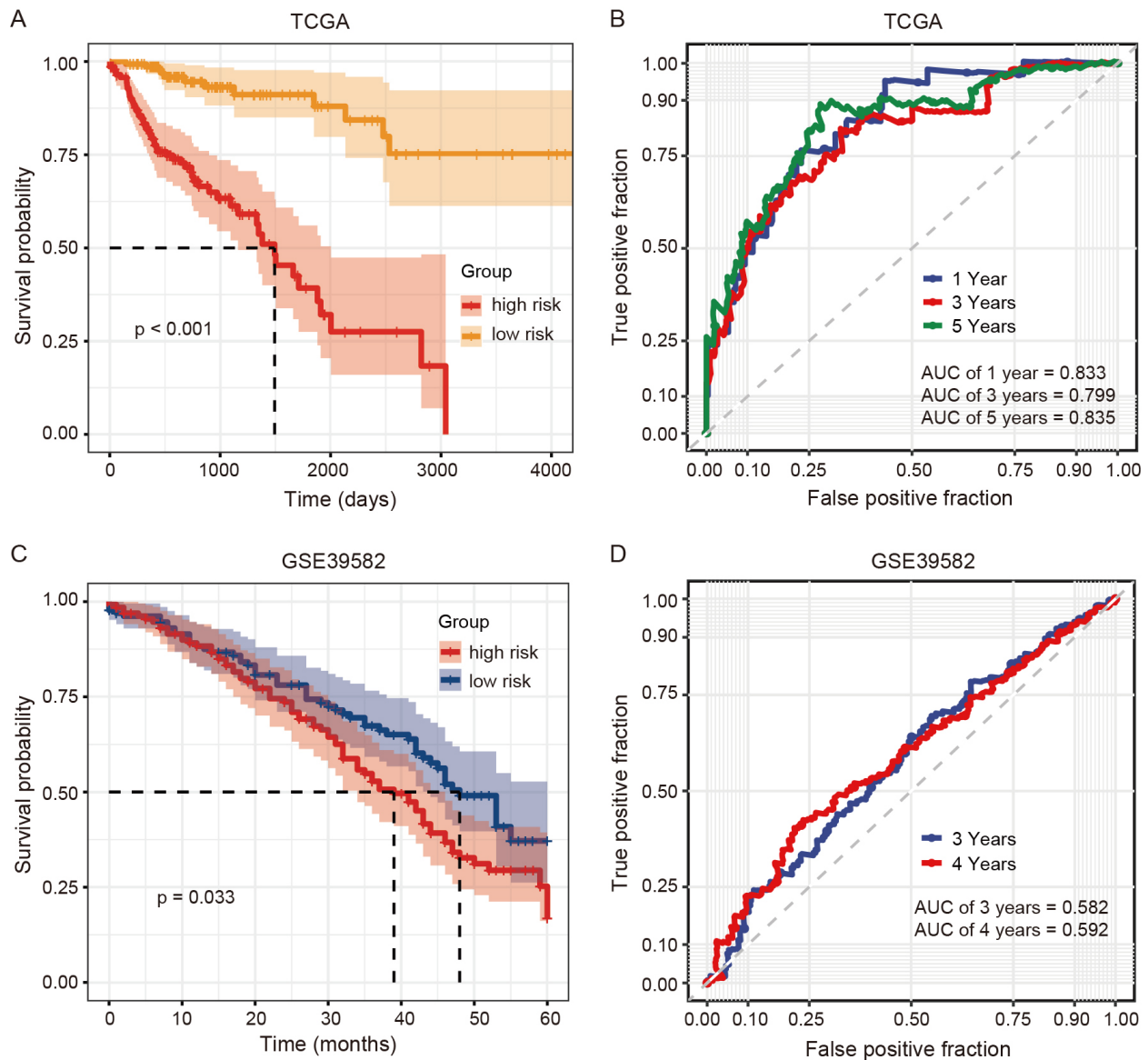


Fig. 4. Predictive efficacy of ferroptosis-related mRNA signatures in COAD patients from The Cancer Genome Atlas (TCGA) and Gene Expression Omnibus (GEO) databases. (A,B) Survival and receiver operating characteristic (ROC) curves of the 12-DE-mRNA signature in COAD patients from the TCGA. (C,D) Survival and ROC curves of the 12-DE-mRNA signature in COAD patients from GSE39582.

4. Discussion

Ferroptosis, an iron-dependent form of programmed cell death, is characterized by intracellular accumulation of lipid peroxidation [28]. Mounting evidence has shown that ferroptosis plays an important role in the pathogenesis of various diseases, especially tumors [29]. An increase in ferroptosis activity has also been shown to suppress the progression of various cancers, such as COAD [30]. Therefore, ferroptosis-related regulatory features at multi-omics levels could potentially be harnessed for cancer diagnosis, classification, and treatment.

In this study, the ferroptosis activity (viz., FS) of each COAD patient was estimated using ssGSEA based on the

expression of 20 ferroptosis-related genes linked to COAD survival, many of which are implicated in tumor pathogenesis. *GPX4*, a well-known oncogene that inhibits ferroptosis in cancer cells [31], showed a negative association with COAD survival ($p < 0.05$), while *FBXW7*, a critical tumor suppressor gene [32], exhibited a positive association with COAD survival ($p < 0.05$). Further analyses also revealed that the estimated FSs were positively associated with COAD survival and negatively associated with COAD pathological stage. These observations suggest the existence of a close relationship between ferroptosis and COAD development.

Enrichment analysis was further conducted to explore the biological functions of protein-coding mRNA genes

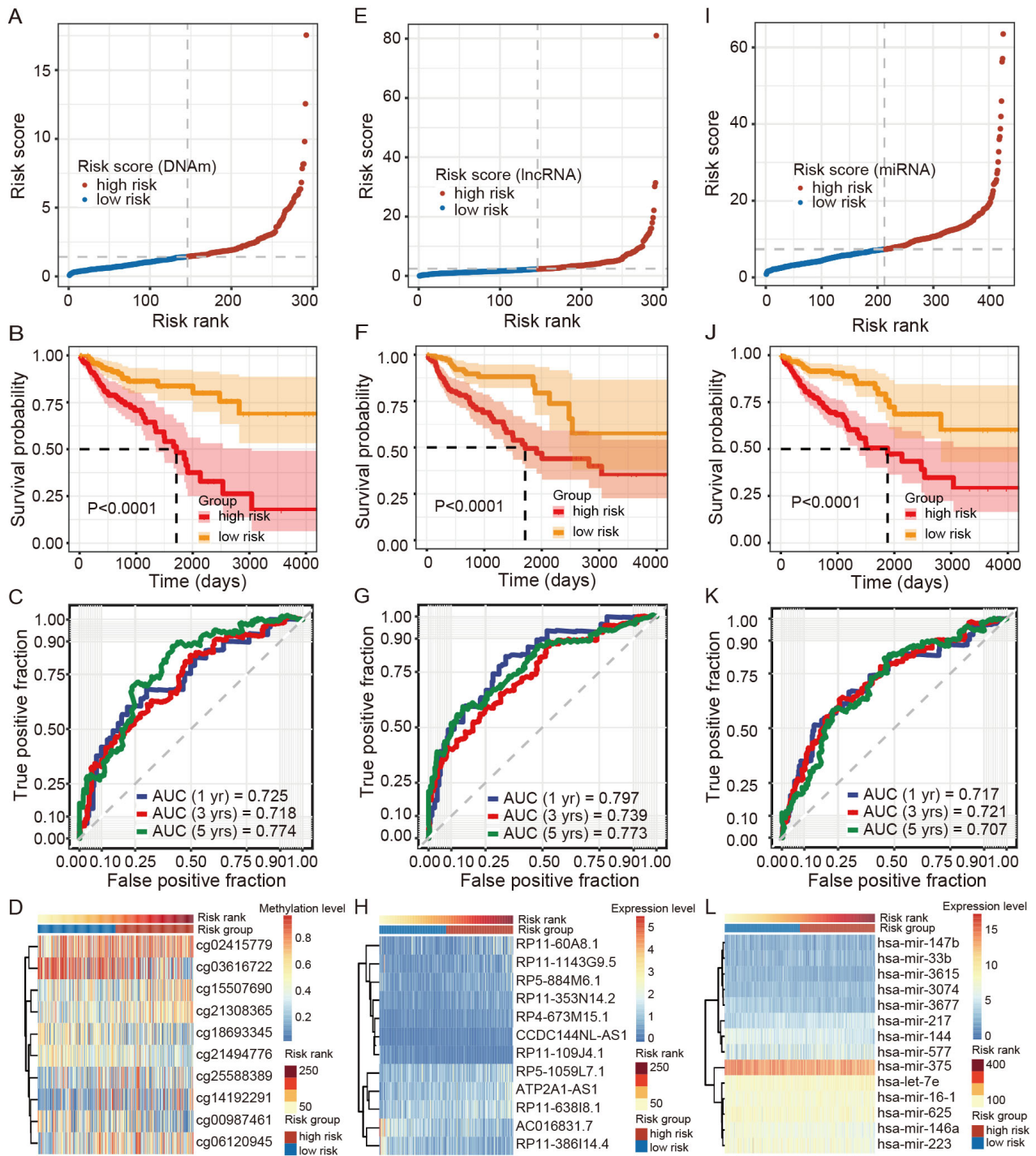


Fig. 5. Construction of ferroptosis-related multi-omics signatures (10 differentially methylated CpG sites (DMCs), 12 DE-lncRNAs, and 14 DE-miRNAs) in COAD patients. (A–D) Risk score plot, survival curve, ROC curve, and heatmap plot of 10-DMC signatures. (E–H) Risk score plot, survival curve, ROC curve, and heatmap plot of 12-DE-lncRNA signatures. (I–L) Risk score plot, survival curve, ROC curve, and heatmap plot of 14 DE-miRNA signatures. In this panel, figures (C,G,K) show predictive performance of three molecular signatures for COAD survival.

that exhibited differential expression between the high- and low-FS COAD subgroups. Results showed that the up-regulated DE-mRNAs were enriched in the TNF signaling, chemokine signaling, and cytokine-cytokine receptor in-

teraction pathways, while the down-regulated DE-mRNAs were enriched in the cell adhesion molecule, chemical carcinogenesis, and cAMP signaling pathways. Several of these pathways, especially those related to immunity, are

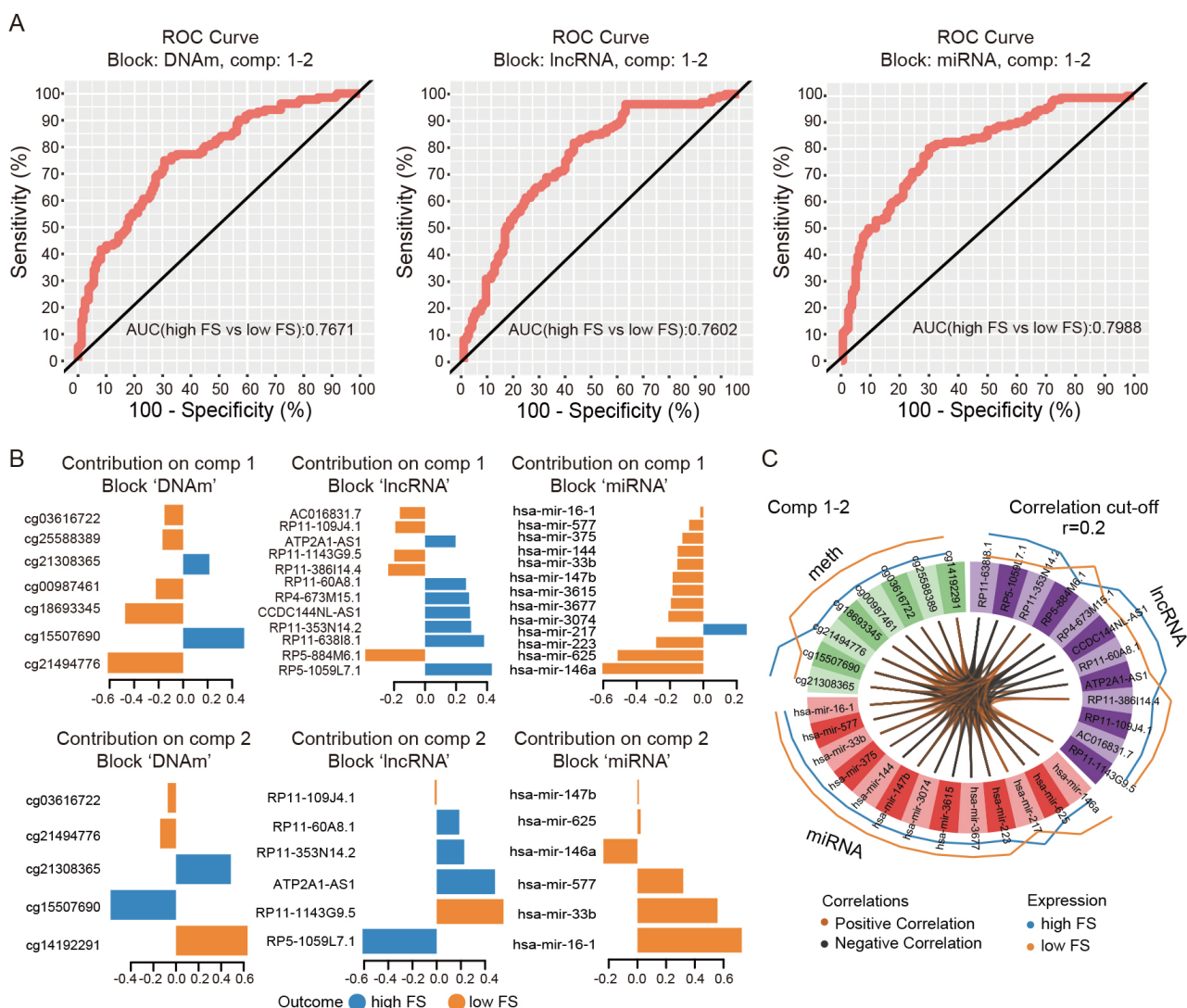


Fig. 6. Discriminant analysis of COAD patients. (A) ROC curves of three molecular signatures (viz., DNAm, lncRNA, and miRNA) discriminating between high- and low-FS patients. Plot suggests that variables (i.e., markers) selected by sparse Partial Least Square-Discriminant Analysis (sPLS-DA) on components 1 and 2 in each of the signatures can discriminate high-FS samples from low-FS samples. (B) Loading weight plots of variables selected by sPLS-DA on components 1 and 2 in each signature. Variables are ranked according to their loading weight (most important at bottom to least important at top). Colors indicate group for which a particular variable has a higher value than the other group. (C) Circos plot of positive or negative correlations between selected variables from three signatures (presented by brown and black links, respectively). Plot represents correlations greater than 0.2 between variables of different molecular types. Outer lines show levels of each variable in the two groups (i.e., high-FS vs. low-FS).

correlated with ferroptosis and cancer development. For example, CD8⁺ T cells can release TNF and interferon gamma (IFN- γ) to drive ferroptosis activity and tumor cell death [33]. In addition, chemokines and cytokines, which are closely related to inflammation, can affect ferroptosis and tumor progression [34,35]. These findings suggest a complex interplay between ferroptosis and the tumor immune microenvironment in the pathogenesis of COAD.

Ferroptosis-related multi-omics signatures at the DNAm, lncRNA, and miRNA levels were identified to predict COAD prognosis, yielding 10 DMCs, 12 DE-lncRNAs,

and 14 DE-miRNAs, respectively. The ROC and AUC results demonstrated the potential of these signatures in predicting COAD survival (AUC >0.7). Notably, patients with high-risk scores derived from the three -omics signatures displayed significantly poorer survival. Moreover, mixOmics analysis revealed that variables from the three -omics datasets were internally correlated and effectively discriminated between the high-FS and low-FS COAD subgroups (all AUC >0.7). A ferroptosis-associated 12-DE-mRNA signature was also constructed based on the transcriptomic data of COAD patients from the TCGA. All

though its predictive accuracy was slightly lower (AUC \approx 0.6) in an independent COAD cohort, possibly due to differences in platforms (RNA-seq vs. microarray), it still supported the relationship between the identified molecular features and COAD prognosis. Collectively, these results suggest that the multi-omics signatures are valuable markers for prognostic assessment and molecular classification in COAD patients.

5. Conclusions

Multiple significant methylation sites, lncRNAs, and miRNAs associated with ferroptosis activity were identified, demonstrating potential as biomarkers for COAD prognosis and classification. These ferroptosis-related multi-omics signatures offer novel clinical perspectives for COAD diagnosis and therapy. Additionally, this study identified a potential relationship between ferroptosis and the immune response, revealing a possible interplay in the development of COAD.

Abbreviations

COAD, colon adenocarcinoma; TCGA, the Cancer Genome Atlas; FS, ferroptosis score; ssGSEA, single-sample gene set enrichment analysis; DNAm, DNA methylation; DE-mRNA, differentially expressed mRNA; DE-lncRNA, differentially expressed lncRNA; DMC, differentially methylated CpG site; DE-miRNA, differentially expressed miRNA; LASSO, least absolute shrinkage and selection operator; ROC, receiver operating characteristic; AUC, area under ROC curve; TNF, tumor necrosis factor.

Availability of Data and Materials

Multi-omics data for COAD samples were downloaded from the TCGA database using the UCSC Xena platform (<https://xena.ucsc.edu/>). An independent gene expression microarray dataset for COAD were downloaded from the Gene Expression Omnibus (GEO) database (GSE39582) (<https://ncbi.nlm.nih.gov/geo/>). All data analyzed during this study are included in this published article.

Author Contributions

YFL and XQC conceived and designed the project and reviewed and approved the manuscript. XQC, KL, and ZWC conducted data analysis and drafted the manuscript. FHX provided valuable assistance and guidance throughout the data acquisition, analysis and interpretation phases of the work. XZ, TL, TW, TS, XYC, and XSC contributed to the interpretation of data derived from the reviewed literature. All authors contributed to editorial changes in the manuscript. All authors read and approved the final manuscript. All authors have participated sufficiently in the work and agreed to be accountable for all aspects of the work.

Ethics Approval and Consent to Participate

This study is based on open-source data obtained from the TCGA and GEO databases, and does not contain any experiments with human participants or animals performed by the authors. All procedures were carried out in accordance with relevant guidelines and regulations. The study was approved by the Institutional Review Board of Colorectal Cancer Clinical Research Center, Third Affiliated Hospital, Kunming Medical University, China (KYCS2023-031).

Acknowledgment

We would like to thank Dr. Christine Watts for help in editing the manuscript.

Funding

This work was supported by a grant from Scientific Research Fund Project of Yunnan Provincial Department of Education (2023Y0657).

Conflict of Interest

The authors declare no conflict of interest.

Supplementary Material

Supplementary material associated with this article can be found, in the online version, at <https://doi.org/10.31083/j.fbl2901013>.

References

- [1] Barderas R, Babel I, Casal JI. Colorectal cancer proteomics, molecular characterization and biomarker discovery. *Proteomics. Clinical Applications*. 2010; 4: 159–178.
- [2] Sung H, Ferlay J, Siegel RL, Laversanne M, Soerjomataram I, Jemal A, *et al.* Global Cancer Statistics 2020: GLOBOCAN Estimates of Incidence and Mortality Worldwide for 36 Cancers in 185 Countries. *CA: A Cancer Journal for Clinicians*. 2021; 71: 209–249.
- [3] Chen W, Zheng R, Baade PD, Zhang S, Zeng H, Bray F, *et al.* Cancer statistics in China, 2015. *CA: a Cancer Journal for Clinicians*. 2016; 66: 115–132.
- [4] Ye L, Zhang T, Kang Z, Guo G, Sun Y, Lin K, *et al.* Tumor-Infiltrating Immune Cells Act as a Marker for Prognosis in Colorectal Cancer. *Frontiers in Immunology*. 2019; 10: 2368.
- [5] McGranahan N, Swanton C. Biological and therapeutic impact of intratumor heterogeneity in cancer evolution. *Cancer Cell*. 2015; 27: 15–26.
- [6] Janney A, Powrie F, Mann EH. Host-microbiota maladaptation in colorectal cancer. *Nature*. 2020; 585: 509–517.
- [7] Kronborg O, Jørgensen OD, Fenger C, Rasmussen M. Randomized study of biennial screening with a faecal occult blood test: results after nine screening rounds. *Scandinavian Journal of Gastroenterology*. 2004; 39: 846–851.
- [8] Xie Y, Hou W, Song X, Yu Y, Huang J, Sun X, *et al.* Ferroptosis: process and function. *Cell Death and Differentiation*. 2016; 23: 369–379.
- [9] Liang JY, Wang DS, Lin HC, Chen XX, Yang H, Zheng Y, *et al.* A Novel Ferroptosis-related Gene Signature for Overall Survival Prediction in Patients with Hepatocellular Carcinoma. *International Journal of Biological Sciences*. 2020; 16: 2430–2441.
- [10] Li L, Qiu C, Hou M, Wang X, Huang C, Zou J, *et al.* Ferroptosis

in Ovarian Cancer: A Novel Therapeutic Strategy. *Frontiers in Oncology*. 2021; 11: 665945.

- [11] Wang Y, Xia HB, Chen ZM, Meng L, Xu AM. Identification of a ferroptosis-related gene signature predictive model in colon cancer. *World Journal of Surgical Oncology*. 2021; 19: 135.
- [12] Wu ZH, Tang Y, Yu H, Li HD. The role of ferroptosis in breast cancer patients: a comprehensive analysis. *Cell Death Discovery*. 2021; 7: 93.
- [13] Zhang X, Huang Z, Xie Z, Chen Y, Zheng Z, Wei X, *et al*. Homocysteine induces oxidative stress and ferroptosis of nucleus pulposus via enhancing methylation of GPX4. *Free Radical Biology & Medicine*. 2020; 160: 552–565.
- [14] Zhang K, Wu L, Zhang P, Luo M, Du J, Gao T, *et al*. miR-9 regulates ferroptosis by targeting glutamic-oxaloacetic transaminase GOT1 in melanoma. *Molecular Carcinogenesis*. 2018; 57: 1566–1576.
- [15] Xie B, Guo Y. Molecular mechanism of cell ferroptosis and research progress in regulation of ferroptosis by noncoding RNAs in tumor cells. *Cell Death Discovery*. 2021; 7: 101.
- [16] Hong Z, Tang P, Liu B, Ran C, Yuan C, Zhang Y, *et al*. Ferroptosis-related Genes for Overall Survival Prediction in Patients with Colorectal Cancer can be Inhibited by Gallic acid. *International Journal of Biological Sciences*. 2021; 17: 942–956.
- [17] Marisa L, de Reyniès A, Duval A, Selves J, Gaub MP, Vescovo L, *et al*. Gene expression classification of colon cancer into molecular subtypes: characterization, validation, and prognostic value. *PLoS Medicine*. 2013; 10: e1001453.
- [18] Zhou N, Bao J. FerrDb: a manually curated resource for regulators and markers of ferroptosis and ferroptosis-disease associations. *Database: the Journal of Biological Databases and Curation*. 2020; 2020: baaa021.
- [19] Hänzelmann S, Castelo R, Guinney J. GSVA: gene set variation analysis for microarray and RNA-seq data. *BMC Bioinformatics*. 2013; 14: 7.
- [20] Yang W, Soares J, Greninger P, Edelman EJ, Lightfoot H, Forbes S, *et al*. Genomics of Drug Sensitivity in Cancer (GDSC): a resource for therapeutic biomarker discovery in cancer cells. *Nucleic Acids Research*. 2013; 41: D955–61.
- [21] Iorio F, Knijnenburg TA, Vis DJ, Bignell GR, Menden MP, Schubert M, *et al*. A Landscape of Pharmacogenomic Interactions in Cancer. *Cell*. 2016; 166: 740–754.
- [22] Maeser D, Gruener RF, Huang RS. oncoPredict: an R package for predicting *in vivo* or cancer patient drug response and biomarkers from cell line screening data. *Briefings in Bioinformatics*. 2021; 22: bbab260.
- [23] Huang DW, Sherman BT, Lempicki RA. Systematic and integrative analysis of large gene lists using DAVID bioinformatics resources. *Nature Protocols*. 2009; 4: 44–57.
- [24] Rohart F, Gautier B, Singh A, Lê Cao KA. mixOmics: An R package for 'omics feature selection and multiple data integration. *PLoS Computational Biology*. 2017; 13: e1005752.
- [25] Auyeung KKW, Law PC, Ko JKS. Combined therapeutic effects of vinblastine and Astragalus saponins in human colon cancer cells and tumor xenograft via inhibition of tumor growth and proangiogenic factors. *Nutrition and Cancer*. 2014; 66: 662–674.
- [26] del Solar V, Lizardo DY, Li N, Hurst JJ, Brais CJ, Atilla-Gokcumen GE. Differential Regulation of Specific Sphingolipids in Colon Cancer Cells during Staurosporine-Induced Apoptosis. *Chemistry & Biology*. 2015; 22: 1662–1670.
- [27] Lin Q, Ma L, Wang D, Yang Z, Wang J, Liu Z, *et al*. A novel Camptothecin analogue inhibits colon cancer development and downregulates the expression of miR-155 *in vivo* and *in vitro*. *Translational Cancer Research*. 2017; 6: 511–520.
- [28] Minagawa S, Yoshida M, Araya J, Hara H, Imai H, Kuwano K. Regulated Necrosis in Pulmonary Disease. A Focus on Necroptosis and Ferroptosis. *American Journal of Respiratory Cell and Molecular Biology*. 2020; 62: 554–562.
- [29] Qiu Y, Cao Y, Cao W, Jia Y, Lu N. The Application of Ferroptosis in Diseases. *Pharmacological Research*. 2020; 159: 104919.
- [30] Li J, Cao F, Yin HL, Huang ZJ, Lin ZT, Mao N, *et al*. Ferroptosis: past, present and future. *Cell Death & Disease*. 2020; 11: 88.
- [31] Zhang X, Sui S, Wang L, Li H, Zhang L, Xu S, *et al*. Inhibition of tumor propellant glutathione peroxidase 4 induces ferroptosis in cancer cells and enhances anticancer effect of cisplatin. *Journal of Cellular Physiology*. 2020; 235: 3425–3437.
- [32] Yeh CH, Bellon M, Nicot C. FBXW7: a critical tumor suppressor of human cancers. *Molecular Cancer*. 2018; 17: 115.
- [33] Wang W, Green M, Choi JE, Gijón M, Kennedy PD, Johnson JK, *et al*. CD8⁺ T cells regulate tumour ferroptosis during cancer immunotherapy. *Nature*. 2019; 569: 270–274.
- [34] Waldmann TA. Cytokines in Cancer Immunotherapy. *Cold Spring Harbor Perspectives in Biology*. 2018; 10: a028472.
- [35] Ozga AJ, Chow MT, Luster AD. Chemokines and the immune response to cancer. *Immunity*. 2021; 54: 859–874.